J. Biomed. Eng. Res.
Vol.26, No.1, 37-42, 2005

Microscopic Imaging of Articular Cartilage using Polarization-Sensitive Optical Coherence Tomography

Sang-Won Lee[1], Jung-Taek Oh[2], Beop-Min Kim[1]

[1]Department of Biomedical Engineering, College of Health Sciences, Yonsei University
[2]Institute for Medical Engineering, Yonsei University
(Received October 4, 2004. Accepted January 3, 2005)

Abstract: We construct and test the polarization-sensitive optical coherence tomography (PS-OCT) system for imaging porcine and human articular cartilages. PS-OCT is a new imaging technology that provides information regarding not only the tissue structures but tissue components that show birefringence such as collagen. In this study, we measure the cartilage thickness of the porcine joint and the phase retardation due to collagen birefringence. Also, we demonstrate that changes of the collagen fiber orientation could be detected by the PS-OCT system. Finally, differences between normal and damaged human articular cartilage are observed using the PS-OCT system, which is then compared with the regular histology pictures. As a result, the PS-OCT system is proven to be effective for diagnosis of the pathology related to the cartilage. In the future, this technology may be used for discrimination of the collagen types. When combined with endoscope technologies, the PS-OCT images may become a useful tool for in vivo tissue testing.

Key words: Polarization-sensitive optical coherence tomography (PS-OCT), Articular cartilage, Collagen fibers, Birefringence

INTRODUCTION

Arthritis is a common degenerative disease that can adversely affect the normal life patterns. Among various types of arthritis, the rheumatoid arthritis may be the most serious one which cause is not yet well defined. It is a chronic inflammatory disease that attacks not only the joint cartilage but other body parts and causes complications such as pleurisy, pericarditis, and disorders in peripheral nerve system. The osteoarthritis is another type of degenerative arthritis that is often seen from the old patients. All types of arthritis cause inflammation and severe pain [1] – [2].

It is important to diagnose the early stage of arthritis before it starts to seriously damage the affected regions. Also monitoring the progress of arthritis is critical for patients who are under certain type of therapy. Conventional methods for monitoring the arthritis include magnetic resonance imaging (MRI), computed tomography (CT) and arthroscopy incorporated with ultrasound. Typical resolutions of MRI and CT are in the range of 100 ㎛, therefore, it is difficult to observe the microscopic changes during invasion of arthritis. Objects as small as 80 ㎛ can be discriminated using the arthroscopy, which is better than MRI or CT. However, only the surface can be seen using the arthroscopy [2]. Recently, the optical coherence tomography (OCT) is drawing much attention as an option that can replace these conventional medical imaging modalities for superficial lesions. OCT can provide cross-sectional images of the scattering media such as biological tissues with resolutions as low as 1 – 15 ㎛. Basic OCT theory is similar to ultrasound B-scan except that it uses light and accordingly, the resolution is much higher [2]-[5]. There are many types of functional OCT technologies including polarization-sensitive OCT (PS-OCT), spectroscopic OCT, Optical Doppler Tomography (ODT), etc. The PS-OCT produces not only the structure cross-sectional image but the functional image regarding the phase retardation and depolarization of light. As a result, the PS-OCT is sensitive to birefringent materials such as collagen, which is full in skin, bone, cartilage, and tooth [6].

We studied the porcine and human articular cartilages using the PS-OCT system. The thickness of

This study was supported by a grant of the Korea Health 21 R&D Project, Ministry of Health and Welfare, Republic of Korea (02-PJ3-PG6-EV07-0002)
Corresponding Author: Beop-Min Kim, Ph.D.
Department of Biomedical Engineering Yonsei University
234 Maeji, Heungup Wonju, Kangwon-Do, 220-710
Tel. (033) 760-2490 Fax. (033) 766-2464
E-mail. beopmkim@dragon.yonsei.ac.kr

cartilage in porcine toe joint was measured. Especially, we showed that different types of cartilages, which are composed of type I and type II collagens, may be discriminated using this technique. Discrimination between different collagen types has clinical importance such as early detection of arthritis. The orientation of the collagen fibers also can be extracted from the PS-OCT images.

The normal and damaged human articular cartilages were examined using the PS-OCT. Comparison with trichrome-stained histology sections prove that the PS-OCT technology may provide *in vivo* histological information on diseases related to cartilage noninvasively.

MATERIALS AND METHODS

Figure 1 shows the schematic of the PS-OCT system configured in this study. OCT is simply a partial coherence Michelson interferometry that produces images similar to the ultrasound B-scans. First, collimated (or fiber-delivered) beam from the broadband light source passes through a linear polarizer which makes the initial light polarization horizontal. Then the beam is incident onto the nonpolarizing beam splitter and split into two arms (reference arm and sample arm). Light in the reference arm passes through a quarter wave plate (QWP) oriented at a 22.5° with respect to the horizontal axis and is reflected by the reference mirror. After the reflected light passes through the QWP again, the light has a 45° linear polarization state. The optical delay in the reference arm is created by using the retro-reflective prism mounted on the rotating galvanometer. The QWP plate in the sample arm is oriented at 45° to horizontal to provide circularly polarized light to the sample. Light reflected from the sample is recombined with light from the reference arm, which produces interference when the optical path length of both arms is within the coherence length of the light source.

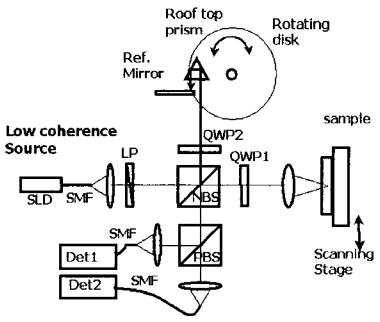

Fig. 1. Schematic of PS-OCT. LP: linear polarizer, PBS: polarization beam splitter, NBS: non-polarization beam splitter, QWP: quater wave plate

Then, lights that are split into two orthogonal polarization states by the polarizing beam splitter are detected by two photodetectors [5]-[8].

The detected signal is digitized by DAQ board and filtered with digital band pass filter. Using Hilbert transformation, we obtain amplitudes and phases, respectively [9]. To determine polarization state of the sample, the Stokes parameters are computed as follows: [5]-[7]

$$\begin{aligned} S_0 &= A_H^2 + A_V^2 \\ S_1 &= A_H^2 - A_V^2 \\ S_2 &= 2A_HA_V\cos(\Delta\alpha) \\ S_3 &= 2A_HA_V\sin(\Delta\alpha),\ \Delta\alpha = \alpha_H - \alpha_V, \end{aligned} \quad (1)$$

where A_H, A_V are the amplitudes, and α_H, α_V are the phases in horizontal and vertical channels, respectively.

Among the four Stokes parameters S_0 is simply the incident irradiance, and S_1, S_2 and S_3 specify the states of polarization. S_1 reflects a tendency for the polarization to be either a horizontal or vertical state. S_2 implies that the polarization of light is close either to +45° or -45° linear states. Finally, S_3 represents a tendency for the light to resemble either right or left circular polarization states [10]. These Stokes parameters obtained by equation (1) represent the polarization states of light immediately after reflection from the sample. Because light reflected from the sample has to pass through QWP oriented at 45° again in the sample arm. The Stokes parameters are exchanged in the detector such that $S_0 \rightarrow S_0$, $S_1 \rightarrow S_3$, $S_2 \rightarrow S_2$, and $S_3 \rightarrow -S_1$ [7]. If the samples are composed of many collagen fibers and possess form birefringence, the Stokes parameters can be rewritten as follows which represent the direction and birefringence of collagen fibers:

$$\begin{aligned} S_0 &\propto R(z) \\ S_1 &= S_0\sin(2\delta(z))\sin(2\phi) \\ S_2 &= S_0\sin(2\delta(z))\cos(2\phi) \\ S_3 &= S_0\cos(2\delta(z)), \end{aligned} \quad (2)$$

where R(z) describes the reflectivity at depth z, $\delta(z)$ is the birefringence, and ϕ is the direction of collagen fibers.

As a light source, we used the superluminescence diode (SLD) that has a center wavelength of 1300 nm and a bandwidth of 40 nm. To verify axial resolution for the system, we used a cover glass and measured the width of the envelope signal from the fringe patterns that are created from the air- glass interfaces. As shown in Figure 2, the axial resolution is approximately 15㎛ in space. To image through certain depth, the galvanometer mirror in the reference arm on which a prism is rotated by 2°,

which gives us the A-scan depth of 2.4 mm. The scanning rate is 20 Hz, the corresponding Doppler (carrier) frequency is 105 kHz and the A-line data points are 5000.

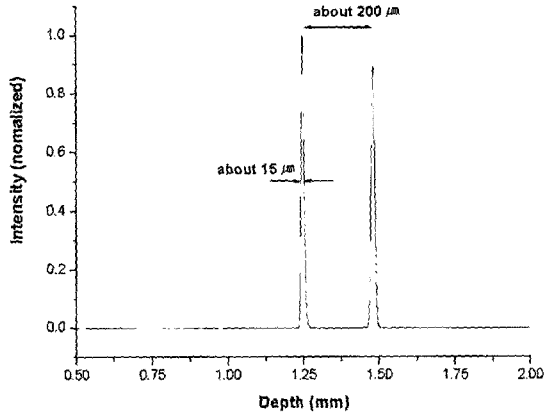

Fig. 2. Estimation of the axial resolution by imaging the cover glass surfaces

RESULTS

Using the PS-OCT system, the condyle of porcine toe was examined. Figure 3(A) shows the S_0 image, which is a cross-sectional structure image of the condyle. The boundary between cartilage (c) and bone (b) is visible in S_0 image. Figure 3(B) is the graph that shows the averaged reflection intensity as a function of depth. From this graph, the thickness of the cartilage layer is measured approximately 0.6 mm which is close to the expected value.

In Figure 4, images that are obtained from a condyle and a meniscus of porcine toe are compared. Three classes of cartilages are known to exist: hyaline cartilage, elastic cartilage and fibrous cartilage. The condyle is a typical hyaline cartilage composed of type II collagen fibers with low birefringence. On the other hand, the meniscus is typical fibrous cartilage that is organized with type I collagen fibers, which is known to possess high birefringence. Figure 4(A) and (B) show images of a condyle, and figure 4(C) and (D) show images of a meniscus. Figure 4 (B) and (D) are S_3 images that show polarization states at the cross-sections. If the polarization state changes fast with depth, band-like fringe patterns are normally visible. Because a condyle has a low birefringence, polarization states are changed slowly as shown in figure 4(B). On the other hand, figure 4(D) shows that polarization states are changed rapidly because the meniscus has a high birefringence.

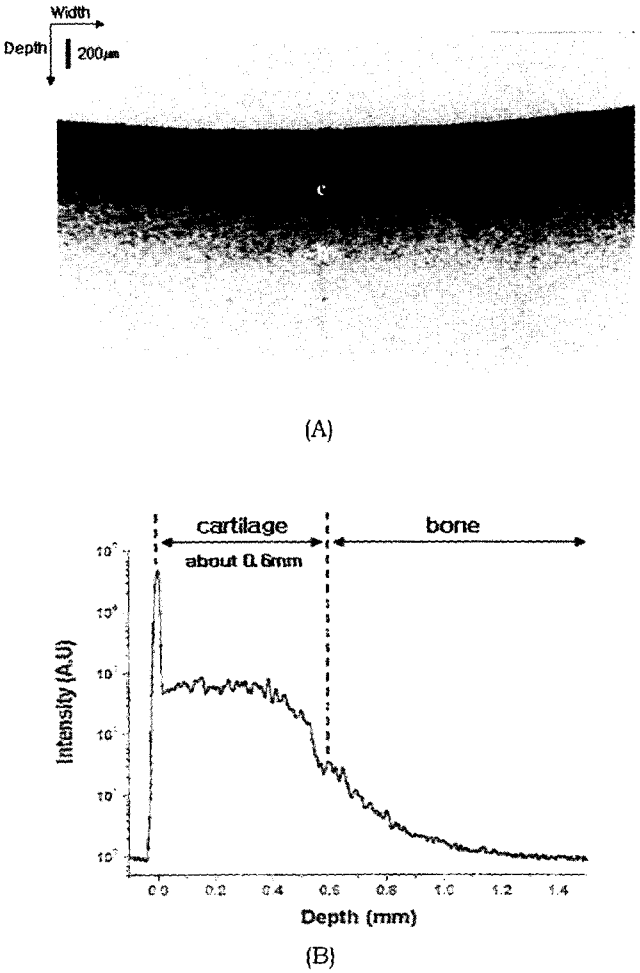

Fig. 3. The condyle measurement of porcine toe. (A) cross-sectional image, (B) averaged intensity graph as a function of the depth.

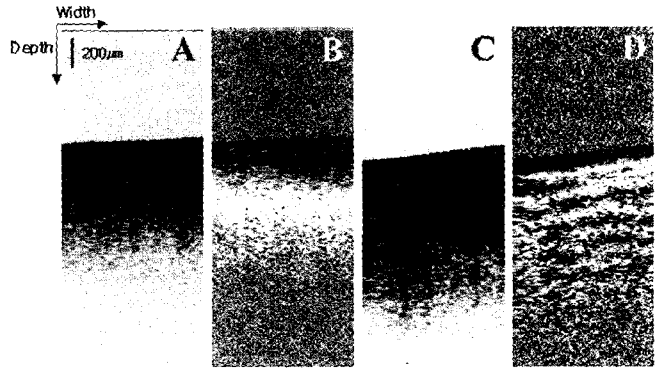

Fig. 4. PS-OCT images of (A) condyle cross-section, (B) condyle polarization, (C) meniscus cross-section, and (D) meniscus polarization

Figure 5 shows the averaged phase changes for condyle and meniscus, which indicates that polarization state of fibrous cartilage changes faster than that of hyaline cartilage. Light is either depolarized or totally attenuated after 0.9 mm depth into the hyaline cartilage and 1.3 mm depth into the fibrous cartilage, respectively. Because the sponge bone contains less-organized collagen contents and has high scattering property, light is immediately depolarized. Therefore, they show that depths of cartilage are respectively 0.9 mm and 1.3 mm.

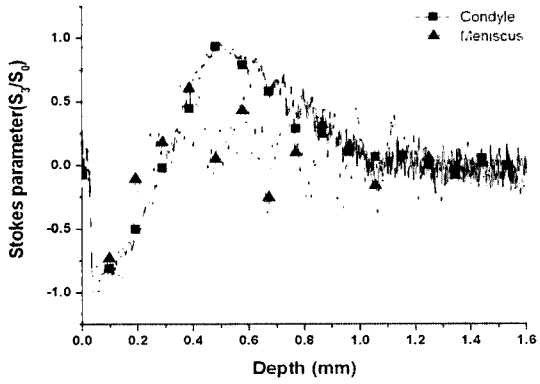

Fig. 5. The polarization state change of different articular cartilages as a function of the depth

Figure 6 is the PS-OCT images that were acquired from different positions of a porcine knee condyle. In this case, due to thick cartilage thickness, the boundary between cartilage and bone are not visible. S_3 images in figure 6(A) and (B) show that patterns of polarization state change are similar, but S_1 and S_2 images indicate that direction of collagen fiber is different from each other. It is more evident from Figure 7(A) and (B), which show the average of the Stokes parameters with depth at each position. between S_2 in figure 7(A) and S_2 in figure 7(B).

A 180° phase shifts exist between S_1 in figure 7(A) and S_1 in figure 7(B), and the same phase shift is observed

Therefore, it is estimated that two directions of collagen fiber is perpendicular. To measure direction of collagen fiber accurately, we use the equation:

$$\varphi = \frac{1}{2}\tan^{-1}\left(\frac{S_1}{S_2}\right) \tag{3}$$

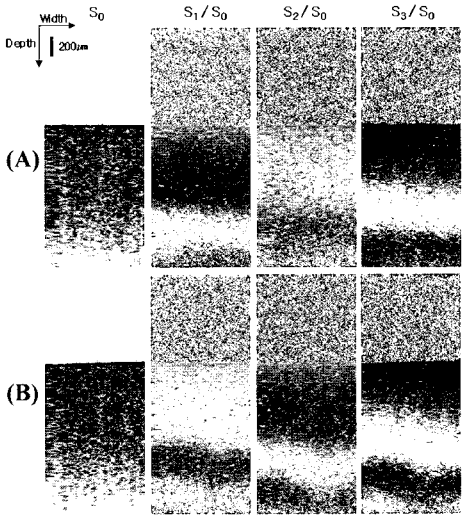

Fig. 6. Stokes parameter images of the condyle at two different locatioons.

Figure 7(C) shows that directions of collagen fiber for figure 7(A) and (B) are about 20° and 110° with respect to the incident light polarization, respectively. Hence, we found that directions of collagen fiber are perpendicular at these two different positions of condyle.

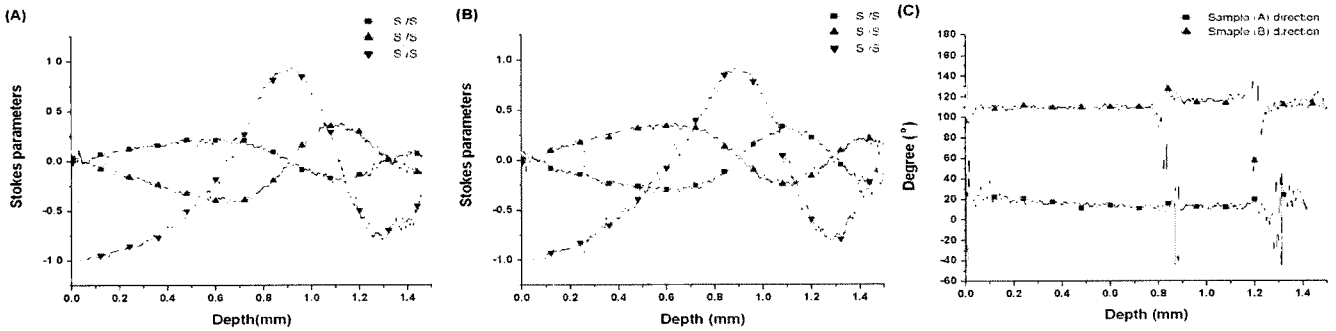

Fig. 7. (A), (B) Averaged Stokes parameter graph of the condyle at two different locations (same locations as Figure 6). (C) Collagen fiber orientations at these two locations

Figure 8 demonstrates the patellar surface of human femur. Figures 8(A), (B) and (C) are intensity image, polarization state image (S_3), and the corresponding histology for normal tissue, respectively. On the other hand, Figures 8(D), (E) and (F) show cross-sectional structure image, polarization state image, and histology for abnormal tissue for worn and damaged cartilage. Because the thickness of cartilage is thick in normal tissue, the layered structure is not visible in figure 8(A). However, polarization state image, S_3, in figure 8(B) shows that polarization state is changed due to birefringence of normal cartilage. Since thickness of cartilage is thin in abnormal tissue, the structure image in Figure 8(D) is similar to histology image [Figure 8(F)]. Also, S_3 image in figure 8(E) shows that polarization change is not visible due to worn out cartilage and bone structure.'

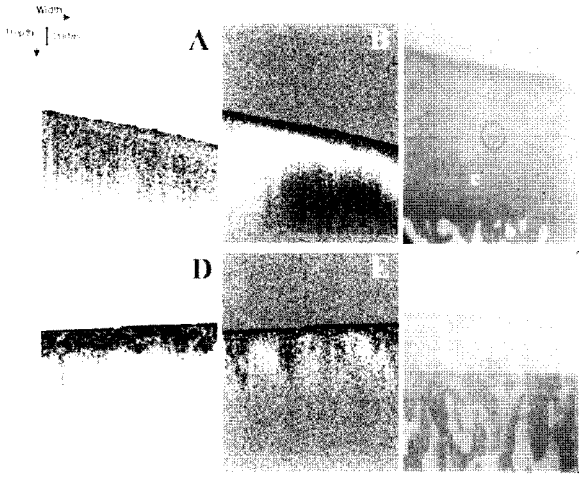

Fig. 8. PS-OCT images of human patellar surfaces on femur side: (A) is the cross-sectional image, (B) is the polarization image and (C) is the histology of the normal tissue, (D) is the cross-sectional image , (B) is polarization image and (C) is the histology of the worn and damaged tissue.

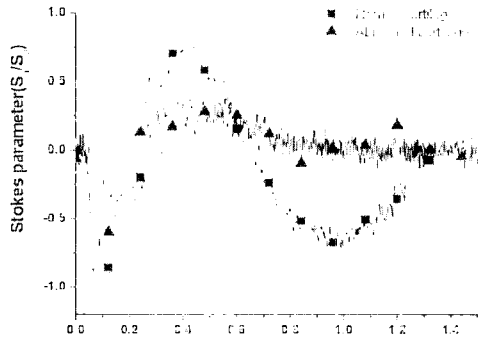

Fig. 9. Polarization state changes for normal and abnormal cartilages of a human as a function of the depth.

CONCLUSION

In this study, the cross-sectional structure and polarization images were obtained. The thickness of toe cartilage was measured and the polarization images between different types of cartilage showed the clear difference. From the S_3 images, it was shown that the phase changes with depth occurs slower for knee condyle (type II collagen) than for meniscus (type I collagen). As a result, we could conclude that the birefringence of type I collagen is stronger than that of type II collagen. The collagen fiber orientation was also can be figured using the PS-OCT system using the S_1 and S_2 images. Finally we tested the PS-OCT system to see if it can produce different images between normal and damaged cartilage tissues. While uniform phase changes are observed in the normal cartilage, the damaged joint contains little cartilage, which is evident by the immediate depolarization and loss of birefringence as seen in the PS-OCT images. The histology studies showed similar cross-sectional pattern between normal and damaged tissues.

As a conclusion, we believe that the PS-OCT system can be a useful tool for diagnosis of arthritis, which may reveal information regarding the healthiness or effectiveness of specific drug. When coupled with endoscope technologies, the PS-OCT may be used for in vivo clinical uses.

REFERENCES

[1] S.H. Lee, Human Anatomy, Hyunmoon, pp. 129-154, 1999.

[2] M.J. Robers, S.B. Adams Jr, N.A. Patel, D.L. Stamper, M.S. Westmore, S.D. Martin, J.G. Fujimoto, and M.E. Brezinski, "*A new approach for assessing early osteoarthritis in the rat*", Analytical and Bioanalytical Chemistry, Vol. 377, No. 6, pp. 1003-1006, 2003.

[3] D. Huang, E.A. Swanson, C.P. Lin, J.S. Schuman, W.G. Stinson, W. Chang, M.R. Hee, T. Flotte, K. Gregory, C.A. Puliafito, and J.G. Fujimoto, "*Optical coherence tomography*", Science, Vol. 254, pp. 1178-1181, 1991.

[4] E.A. Swanson, Optical coherence tomography principles, instrumentation, and biological applications, Biomedical Optical Instrumentation and Laser-Assisted Biotechnology, pp.291-303, 1996.

[5] B.E. Bouma, G.J. Tearney, Handbook of Optical coherence tomography, Marcel Dekker, Inc., 2002.

[6] J.F. de Boer, S.M. Srinivas, B.H. Park, T.H. Pham, Z. Chen, T.E. Milner, and J.S. Nelson, "*Polarization effects in optical coherence tomography of various biological tissues*", IEEE Journal of selected topitcs in quantum electornics, Vol. 5, No. 4, pp. 1200-1204, 1999.

[7] J.F. de Boer, T.E. Milner, "*Review of polarization sensitive optical coherence tomography and Stokes vector determination*", Journal of Biomedical Optics, Vol. 7, No. 3, pp. 359-371, 2002.

[8] H. Ren, Z. Ding, Y. Zhao, J. Miao, J.S. Nelson, and Zhongping Chen, "*Phase-resolved functional optical coherence tomography : simultaneous imaging of in situ tissue structure, blood flow velocity, standard deviation,*

birefringence, and Stokes vectors in human skin", Optics Letters, Vol. 27, No. 19, pp. 1702-1704, 2002.

[9] Y. Zhao, Z. Chen, Z. Ding, H. Ren, and J.S. Nelson, "*Real-time phase-resolved functional optical coherence tomogrphy by use of optical Hilbert transformation*", Optics Letters, Vol. 27, No. 2, pp. 98-100, 2002.

[10] Eugene Hecht, Optics Fourth edition, Addison Wesley, pp. 325-384, 2002.

[11] J.T. Oh, B.M. Kim, and S.W. Kim, "*Statical characteristics of polarization-sensitive optical coherence tomography for tissue imaging*", Journal of the Optical Society of Korea, Vol. 7, No. 4, pp. 211-215, 2003.

[12] C.K. Hitenberger, E. Götzinger, M. Sticker, M. Pircher, and A.F. Fercher, "*Measurement and imaging of birefringence and optic axis orientation by phase resolved polarization sensitive optical coherence tomography*", Optics Express, Vol. 9, No. 13, pp. 780-790, 2001.

[13] M.C. Pierce, J. Strasswimmer, B.H. Park, B. Cense, and J.F. de Boer, "*Birefringence measurements in human skin using polarization-sensitive optical coherence tomography*", Journal of Biomedical Optics, Vol. 9, No. 2, pp. 287-291, 2004.

[14] M.R. Hee, D. Huang, E.A. Swanson, and J.G. Fujimoto, "*Polarization-sensitive low-coherence reflectometer for birefringence characterization and ranging*", Journal of Optical Society of America B, Vol. 9, No. 6, pp. 903-908, 1992.

[15] C.E. Saxer, J.F. de Boer, B.H. Park, Y. Zhao, Z. Chen, and J.S. Nelson, "*High-speed fiber-based polarization-sensitive optical coherence tomography of in vivo human skin*", Optics Letters, Vol. 25, No. 18, pp.1355-1357, 2000.

[16] J. Zhang, S. Guo, W.G. Jung, J.S. Nelson, and Z. Chen, "*Determination of birefringence and absolute optic axis orientation using polarization-sensitive optical coherence tomography with PM fibers*", Optics Express, Vol. 11, No. 24, pp. 3262-2370, 2003.

[17] P.H. Tran, D.S. Mukai, M. Brenner, and Z. Chen, "*In vivo endoscopic optical coherence tomography by use of a rotational microelectromechanical system probe*", Optics Letters, Vol. 29, No. 11, pp. 1236-1238, 2004.